A Binomial Model for Radiated Immunity Measurements

Emmanuel Amador, Hans Georg Krauthäuser, *Senior Member, IEEE,* and Philippe Besnier, *Senior Member, IEEE.*

***Abstract*—We propose a statistical analysis of immunity testing in EMC based on binomial distributions. This approach aims at extracting the immunity properties of a device from its probability of failure during a test. We show that under certain conditions, this approach can be applied to plane wave testing environments and reverberation chambers. This approach allows one to control the uncertainty of the immunity level estimation and to reduce the duration of a test by both reducing significantly the number of observations needed to reach a given uncertainty budget and by giving an optimal number of power level tested. We show the benefits of such approach for immunity testing and we present some experimental results.**

***Index Terms*—Binomial, full anechoic room, immunity, open area test site, optimization, reverberation chamber, statistics, testing.**

I. Introduction

In electromagnetic compatibility (EMC), the outcome of an immunity testing that consists of n observations (angles of incidence and polarizations in a plane wave setup or stirrer positions in a reverberation chamber) is generally binary, the equipment under test (EUT) may pass or fail the test. In this work we propose an alternative approach based on the statistics of the test. We take advantage of the statistical information contained in the n observations performed during the test to draw an accurate picture of the immunity of the EUT.

Plane wave testing environments like fully anechoic rooms (FARs) [1] , open area test sites or guided waves environments like GTEM cells [2] are regarded as deterministic testing environments. But the small number of angles of incidence tested during an EMC qualification (generally less than 20) does not allow to get an exhaustive picture of the immunity of an EUT. Random fields testing environments like reverberation chambers (RC) test a large number of incidence angles simultaneously. They provide a solid alternative for EMC measurements [3] and have grown more and more popular during the last years.

Two kinds of immunity testing are generally performed. A test against a given E-field limit that states if the EUT is able to endure a given field strength or not. And a test to measure the immunity level of an EUT. In this work we focus on the second kind of immunity testing.

The immunity levels obtained with a same EUT in a deterministic environment and a statistical environment can be disparate and a very popular topic in the EMC community is to correlate these two kinds of measurements [4]–[7]. In this article we propose a binomial-based model of the testing that provides a general statistical framework for both plane waves testing environments as long as the EUT meets some requirements and random fields testing environments like RCs. We show that the statistics of a test can be well described with a binomial process and that the uncertainty can be controlled to meet common EMC requirements. This approach allows to reduce the duration of the immunity level measurement by introducing an optimal number of power steps tested for a given number of observations n. Moreover we will show that the immunity levels derived by this approach with random fields are in agreement with measurements performed with plane wave setup.

We first describe the statistics of a test by using a binomial distribution. We discuss different testing scenarios we may encounter in order to define the application domain of this approach. We apply this approach to radiated immunity testing with a Rayleigh statistics and we give the statistical properties of the estimated immunity level. We perform measurements with two different EUTs and show the benefits of such approach in an RC in terms of accuracy of the results, duration of the test and correlation with deterministic testing environments.

II. Statistics of a Test

The statistics of a test is generally studied with binomial distributions. Let x be a binomial random variable. If the probability of failure of the test is p, the probability to observe k failures among n observations is given by the following probability [8]:

$$P\{x = k\} = \binom{n}{k} p^k (1-p)^{n-k}. \tag{1}$$

Studying an EMC test with n observations as a binomial process allows to use more information to extract the immunity properties of an EUT and gives a statistical background for controlling the uncertainty of the estimation.

A. Probability of failure p

1) Estimation of p: Figure 1 shows values of $P\{x = k\}$ for different values of p and k with a total number of $n = 10$

Manuscript received ...

This work is supported by the Direction Générale de l'Armement (DGA), part of the French ministry of defense, through a postdoctoral grant delivered to Emmanuel Amador.

Emmanuel Amador is with the Chair of Electromagnetic Theory and Compatibility, TU Dresden, 01069 Dresden, Germany and with the IETR, UMR CNRS 6164, Université Européenne de Bretagne, Rennes, France, (email: emmanuel.amador@insa-rennes.fr).

Hans Georg Krauthäuser is with the Chair of Electromagnetic Theory and Compatibility, TU Dresden, 01069 Dresden, Germany, (email: hgk@ieee.org).

Philippe Besnier is with the IETR, UMR CNRS 6164, Université Européenne de Bretagne, Rennes, France, (email: philippe.besnier@insa-rennes.fr).

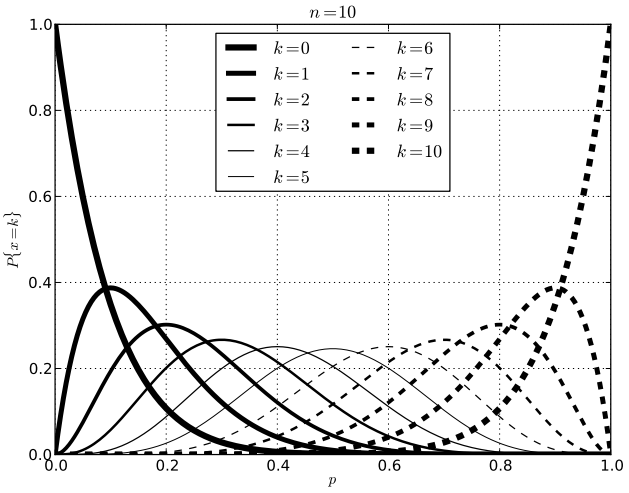

Fig. 1. $P\{x = k\}$ for $n = 10$ and different values of k.

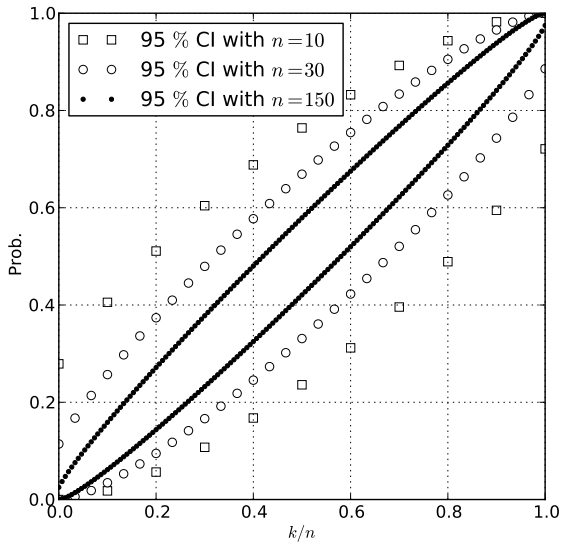

Fig. 2. Confidence interval of p for $n = 10$, 30, 150.

observations. As expected, the maximum of $P\{x = k\}$ is observed for $p = k/n$. This figure shows that the probable range of values of p for a given combination of k and n can be relatively large. Considering a test carried out over n observations and having recorded k failure(s), the estimation of the probability of failure $\hat{p}$ is empirically given by:

$$\hat{p} = \frac{k}{n}. \tag{2}$$

2) Statistics of p: Confidence interval (CI) estimation of binomial distribution is a topic of interest in statistics since 1812 [9]. Many different approaches are given in the literature. Praised "exact solutions" like the Clopper-Pearson interval [10] can be less accurate than approximate solutions as explained in [11]. We will use the Wilson interval [12], recent works [13], [14] seem to agree that this interval is valid for small values of n, unlike the popular normal approximation [8].

If z_γ denotes the half-width of the CI of a normal distribution with 0 mean and variance equal to 1, $\mathcal{N}(0, 1)$, so that $1-\gamma$ percents of the values are in the CI (for example $z_{0.05} \approx 1.96$), the boundaries of p CI are [12] :

$$p_{\min} = \hat{p} + \frac{z_\gamma^2}{2n} - \Delta \tag{3}$$

$$p_{\max} = \hat{p} + \frac{z_\gamma^2}{2n} + \Delta \tag{4}$$

with

$$\Delta = z_\gamma \frac{\sqrt{[\hat{p}(1-\hat{p}) + z_\gamma^2/4n]/n}}{1 + z_\gamma^2/n}.$$

Figure 2 shows the 95 % CI for different values of n and for the different possible values of $k/n = \hat{p}$ computed with (3) and (4). We can note that with typical values of n around 10 or 30, the CI is clearly not centered around $\hat{p}$ with a $\frac{z_\gamma^2}{2n}$ offset and therefore a normal approximation is not relevant. As expected the width of the CI decreases with n. The Wilson interval formulation [12] is used in this work to extract the maximum error estimation during an immunity testing.

III. Description of a radiated immunity testing

In this section we give a general description of a radiated immunity testing in EMC. We will define three essential elements of immunity testing: the nature of the field, the coupling and the susceptibility level. And we will discuss the different combinations of field nature and coupling complexity and their effects on the testing statistics.

A. Fields

We can distinguish two kinds of fields. Deterministic fields are observed in plane wave setups like a FAR, an OATS or a GTEM cell. The magnitude of the rectangular components of these fields impinging the EUT is not statistical and can be derived from the setup parameters (distance, power injected, antenna gain, dimensions of the GTEM cell) or a measurement.

Random fields are observed in RCs. The magnitude of the E-field rectangular components is statistically distributed. In an ideal RC the component magnitude follows a Rayleigh distribution [15], [16].

B. Coupling and susceptibility level

The coupling between the EUT and the E-field can be described with coupling paths. There may be one or several coupling paths between the external field and different parts of the system that will provoke a failure. In this study, we will define the susceptibility level of the EUT by using the magnitude of a rectangular field component impinging on the EUT. If this magnitude is greater than a particular value E_s, we will observe a failure. E_s is the susceptibility level of the EUT. To simplify the study, we will consider that the EUT consists of only one susceptible part. In the general case, several parts of the EUT may provoke a failure.

There may be one or multiple coupling paths between the part that provoke a failure and the external field. The number of coupling paths gives a hint on the complexity of

the EUT's radiation pattern. If the radiation pattern of an EUT is very simple or easily identified, it is easy for the operator performing the test to obtain the worst case when illuminating the EUT. A typical example would be a shielded EUT with an external antenna. In this simple case, the radiation pattern is simple and can be regarded as deterministic.

If the number of coupling paths is important and/or if the EUT is electrically large or resonating, the radiation pattern can be very complex. In [17], the author shows that for electrically large EUTs, the radiated power can be described through well known statistical distributions. The radiated power of such EUT follows an exponential distribution. It means that the rectangular components of the E-field radiated follow a Rayleigh distribution [8]. Appendix A provides a concise alternative proof of this result. The radiation pattern of an EUT is related to its electrical size and its inner complexity. As long as an EUT is electrically large enough and complex enough, the power radiated follows a canonical distribution like an exponential distribution.

C. Different testing scenarios and their complexity

The impinging electric field can either be deterministic or random, the EUT could be simple (like a wire), resonating (with one or multiple apertures) and so the coupling between the external field and the EUT can be either simple or complex. This leads to different scenarios:

- with deterministic E-field:
  - and simple coupling: it can be a simple wire illuminated, a cavity with an aperture or a directive object. In these cases, the worst case is easy to determine and a small number of illuminations (different angles of incidence and polarization) is needed to perform the test. In these situations, the coupling is almost completely deterministic and it is not possible to make n independent observations.
  - and complex coupling: in this case the randomness is provided by the EUT itself. The test can be described as a binomial process. As long as the random distribution that governs the radiation of the EUT is known [17], performing a test with a limited number of observations n may lead to the level of susceptibility of the EUT E_s.
- with random E-field:
  - and simple coupling: the randomness is provided by the impinging E-field. As long as n independent observations can be performed, the test can be described by a binomial process. The case of a cavity with a small aperture studied in [18] gives a double Rayleigh statistic for the rectangular components of the E-field in an RC and with an overmoded cavity as EUT. With a non resonating EUT, the underlying statistics is provided by the impinging E-field and follows a Rayleigh distribution.
  - and complex coupling: the randomness is provided by both the impinging E-field and the radiation pattern of the EUT. In this case, the resulting E-field is the superposition of contributions with their amplitude modulated by independent Rayleigh random variables. The resulting E-field is a Rayleigh distribution [18].

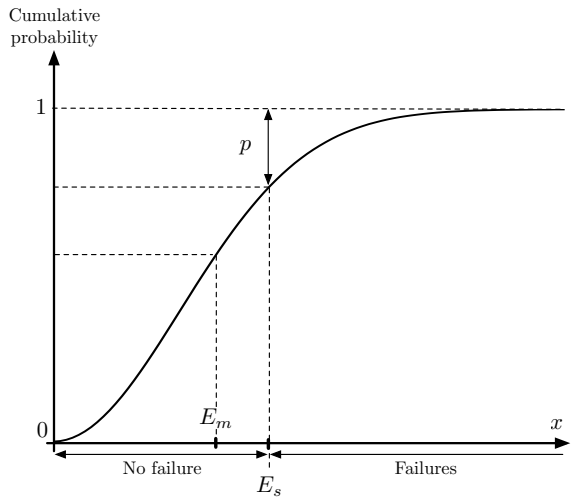

Fig. 3. Cumulative Rayleigh distribution function, the relation between the probability of failure p during a test, the mean magnitude of the E-field component E_m and the susceptibility level E_s is shown.

In most cases, the underlying statistics of the test is governed by a Rayleigh distribution. We will focus on immunity testing with Rayleigh distributed observations in the next section.

IV. Immunity Measurement with Rayleigh Distributed Randomness

In this section, we take advantage of the knowledge of $\hat{p}$ to assess the susceptibility level of an EUT. The probability of failure enables to obtain more information on the susceptibility level of an EUT than the approaches defined in the standards. In plane wave environments [1], [2], the limited number of angles of incidence tested does not allow to extract a complete picture of the EUT's immunity. In an RC, the maximum-based estimation of the susceptibly [3] adds a statistical uncertainty on the levels measured.

Randomness is mandatory in this approach. The number of observations n can be seen as the number of independent incidence angles and polarizations in a plane wave environment or the number of independent stirrer positions in an RC. We will focus on Rayleigh distributed rectangular components of the E-field but any random distribution can be used. Weibull distribution for example may be more convenient to describe the E-field in an RC at low frequencies, empirical distribution retrieved from measurements can be used too as long as n independent observations can be made. We note n the total number of measurements and k the number of measurements that present a failure.

A. Relation between the probability of failure p and the susceptibility level E_s of the EUT

Let an EUT have a susceptibility level E_s. We consider that the magnitude of the rectangular components of the impinging

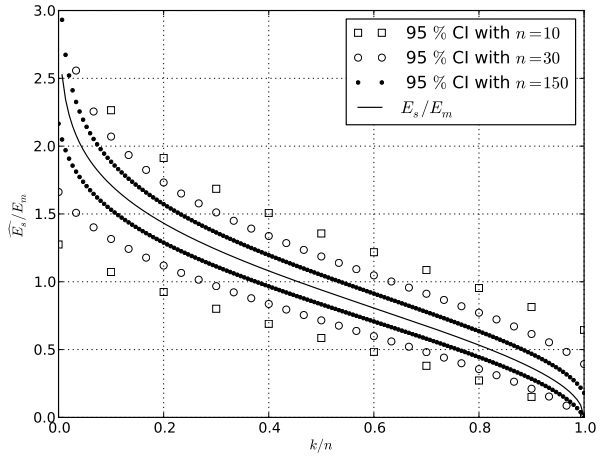

Fig. 4. Confidence interval of $\widehat{E_s}/E_m$ for $n = 10$, 30, 150.

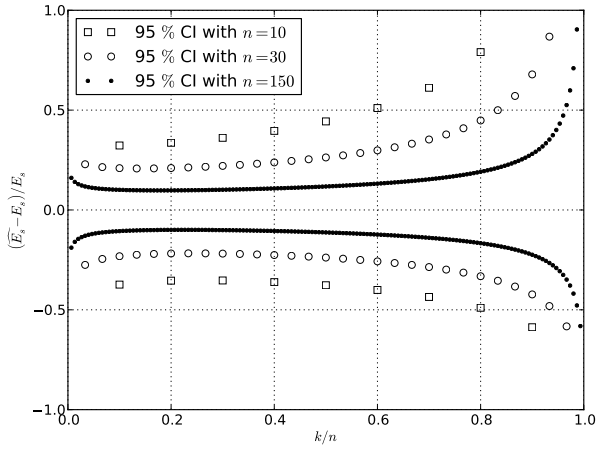

Fig. 5. Estimation error: $\varepsilon = \left(\widehat{E_s} - E_s\right)/E_s$ for $n = 10$, 30, 150.

E-field follows a Rayleigh distribution. The probability density function of the random variable X that follows a Rayleigh distribution with scale parameter σ is given by [8]:

$$f_X(x) = \frac{x}{\sigma^2} e^{-x^2/2\sigma^2}, \text{ with } x \geq 0, \tag{5}$$

X is the random variable that corresponds to the magnitude of a rectangular component of the E-field. The probability p to observe a failure is given by the condition $X > E_s$ as depicted in figure 3. This probability is given by:

$$p = 1 - F_X(E_s) = e^{-E_s^2/2\sigma^2}, \tag{6}$$

where F_X is the cumulative distribution function of X. Without loss of generality, we can use the mean value[1] $E_m = \sigma\sqrt{\pi/2}$ of a rectangular component of the E-field and thus:

$$p = e^{-\frac{\pi}{4}\left(\frac{E_s}{E_m}\right)^2}, \tag{7}$$

we can derive the level of susceptibility of an EUT as a function of p and E_m:

$$E_s \quad = \quad 2E_m\sqrt{\frac{\ln(1/p)}{\pi}}. \tag{8}$$

B. Statistics of E_s

In this part, we use the Wilson CI formulation [12] of p to derive the statistics of E_s. Because (8) is a monotonically decreasing function of $\hat{p}$, the derivation is straightforward. By using the Wilson CI (3) (4), we can derive the CI of $\widehat{E_s}/E_m$ by computing $\widehat{E_s}(p_{\min})/E_m$ and $\widehat{E_s}(p_{\max})/E_m$, where $\widehat{E_s}$ is the estimator of E_s. Figure 4 shows the ratio E_s/E_m versus p. We can see that for low values of the probability of failure $\hat{p}$ this approach could allow to detect susceptibilities that are twice the value of E_m. In terms of power, that represents a gap of around 6 dB. The CI of E_s for $n = 10$, 30 and 150 are given in figure 4.

Figure 5 shows the relative error estimation $\varepsilon = (\widehat{E_s} - E_s)/E_s$. The error is greater for values of $\hat{p}$ that are near 1 than for values of $\hat{p}$ near 0, this is mainly due to the relation between E_s and p (8). Choosing values of $\hat{p} = k/n$ between 0.1 and 0.6 with $n = 10$, guarantees that the maximum absolute error ε_M for 95% of the values is smaller than 50 %. A 50 % error on a field component is almost a 3 dB error in terms of power. This result indicates that this statistical estimation of the susceptibility level does not specifically require high test levels. With $n = 150$ and $\hat{p}$ between $1/150$ and 0.8 the the maximum absolute error ε_M, is under 20 %.

[1]In an RC E_m can be derived from the quality factor and the power injected. In a plane wave setup, it should be estimated during the test or derived from the measurement setup.

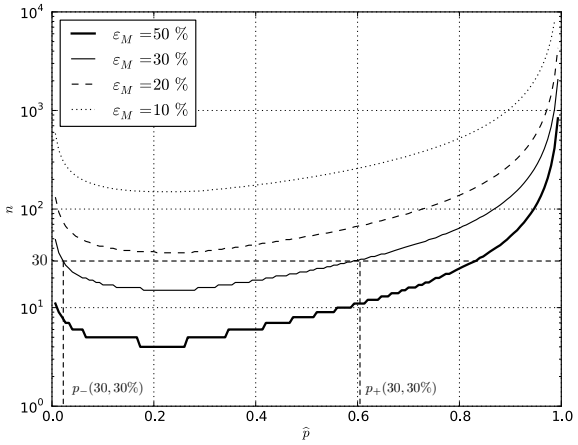

Fig. 6. Number of measurements n needed to achieve a maximum error budget ε_M of 50%, 30%, 20%, 10% for different values of $\hat{p}$. p_- and p_+ are given for $n = 30$ and $\varepsilon_M = 30\%$.

Wilson intervals allow to access very easily the maximum error of an estimation and can be associated to any measurement. It can be helpful during a measurement to estimate the uncertainty on the fly. As long as n and $\hat{p}$ do not allow to reach a given uncertainty budget for $\widehat{E_s}$, the number of observations n can be increased.

Figure 6 gives the number of measurements needed to achieve a given maximum error for different values of $\hat{p}$. This curve gives the range $[p_-; p_+]$ of values that allows to achieve a given error budget with a given number of measurements n. For example, to reach an uncertainty budget lower than 50 %,

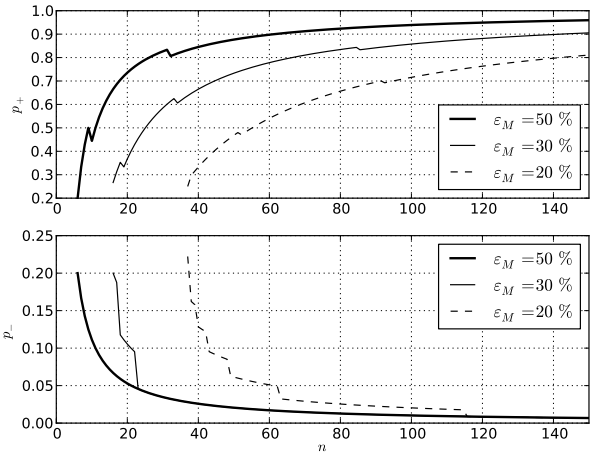

Fig. 7. Values of p_+ and p_- vs. n for different error budgets.

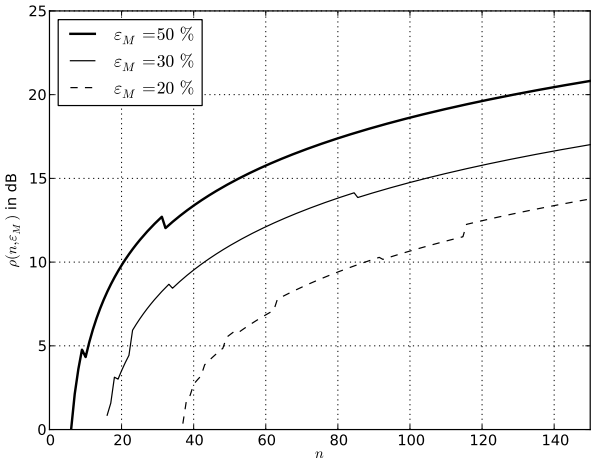

Fig. 8. $\rho(n, \varepsilon_M)$ vs. n for different error budgets.

it means that $\varepsilon_M < 50\%$ with $n = 10$ we can predict E_s with values of $\hat{p}$ from $p_- = 0.1$ to $p_+ = 0.6$.

Figure 7 shows the values of p_+ and p_- for different uncertainty budgets computed with the Wilson interval. These values are particularly useful for an immunity testing as they provide the range of value of E_s that are tested for a given level of injected power and a given number of observations n.

C. Relation between the number of observations n and the number of power levels tested n_p

Knowing $p_-(n, \varepsilon_M)$ and $p_+(n, \varepsilon_M)$, defined for a given number of measurements n and a maximal error budget ε_M according to Wilson CI (3) and (4) gives the range of susceptibility tested. This range is between:

$$2E_m\sqrt{\frac{\ln(1/p_+(n,\varepsilon_M))}{\pi}} \leq E_s \leq 2E_m\sqrt{\frac{\ln(1/p_-(n,\varepsilon_M))}{\pi}} \tag{9}$$

In the standards, the set of power levels tested is defined without regard to the number of observations n. With this binomail approach, if n increases, the interval $[p_-; p_+]$ widens and the range of values of E_s tested increases. We can establish a relation between n and the number of power levels tested during a test n_p. Let name E_{m_i} the ith mean value of the E-field in the chamber corresponding to the i-th level of power injected in the chamber. The successive levels tested E_{m_i} can be derived from (9) by the following geometric sequence:

$$E_{m_{i+1}} \approx E_{m_i}\sqrt{\frac{\ln(p_-(n,\varepsilon_M))}{\ln(p_+(n,\varepsilon_M))}}, \tag{10}$$

and thus:

$$\begin{aligned} E_{m_i} &= E_{m_0}\left(\sqrt{\frac{\ln(p_-(n,\varepsilon_M))}{\ln(p_+(n,\varepsilon_M))}}\right)^i \\ E_{m_i} &= E_{m_0}\rho^i(n,\varepsilon_M), \end{aligned} \tag{11}$$

where E_{m_0} is the first level tested. This sequence gives the optimal set of mean magnitude E_{m_i} used during the test and thus allows to reduce the test's duration. With $n = 10$ and $\varepsilon_M = 50$ %, $\rho(n, \varepsilon_M) \approx 1.8$, in terms of power it represents a +5 dB step between successive power levels.

Figure 8 gives the values of the steps in dB one should respect for any number measurements n and for three different error budgets ε_M. By using an optimal number of level tested, one can reduce the test's duration without sacrificing the accuracy of the estimation.

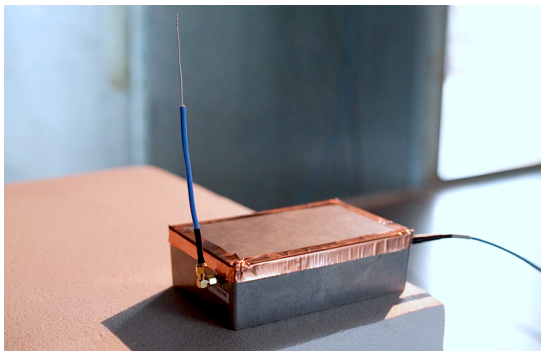

Fig. 9. External view of the simple EUT.

V. Measurements

We present here some measurements performed in an RC and in a GTEM cell. These measurements were performed in the EMC lab at IETR in Rennes. The GTEM cell at IETR is a Teseq GTEM 500 and the dimensions of the RC are $8.7 \times 3.7 \times 2.9$ m^3. Due to a lack of available power, measurements in a FAR with the same EUTs could not be performed. We show that the levels extracted with this binomial approach in an RC are in agreement with measurements performed according the GTEM standard [2]. More measurements are planned for future investigations.

A. EUTs

1) Simple EUT: This EUT consists of an electronic board that contains an operational amplifier (op-amp) as a comparator placed in a metallic enclosure. A 5 cm long monopole external antenna is connected to the circuit as shown in

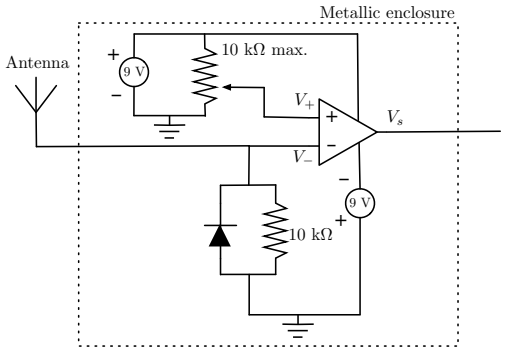

Fig. 10. Schematic view of the simple EUT's electronic board.

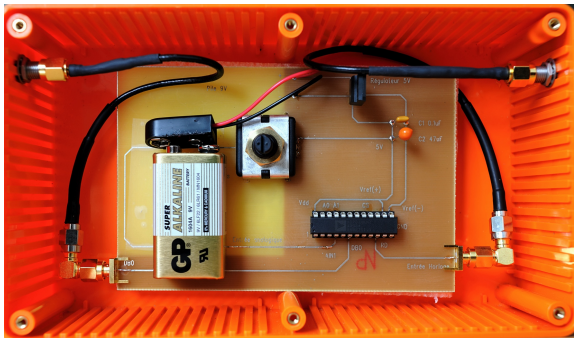

Fig. 11. Internal view of the complex EUT.

figure 9. The coupling path is assured by the monopole antenna only. The worst case scenario in a deterministic testing environment like a GTEM cell is easy to determine.

A schematic of the electronic circuit is given in figure 10. The antenna is associated with an envelope detector for filtering the high frequency disturbances received by the antenna. Without any disturbance, since $V_+ > V_-$ the op-amp delivers $V_s = 9$ V. With disturbances leading to $V_- > V_+$, the op-amp provides $V_s = -9\ V$ indicating a default. The signal V_s is recorded with a digital oscilloscope and a home made program that controls all the experimental setup returns either the value 0 in the case of no susceptibility, or the value 1 if a susceptibility is detected.

2) Complex EUT: This EUT consists of an electronic board that contains an analog to digital converter (ADC), placed in a plastic box. Most of the board does not have a ground plane at the back. There may be several coupling paths between the external field and the board. From 850 MHz to 1500 MHz, the electrical size of the board is varying from $0.4\lambda \times 0.3\lambda$ to $0.75\lambda \times 0.5\lambda$. A photograph of the electronic board is given in figure 11. The radiation pattern complexity of the EUT is increasing with the frequency as more and more parts of the circuit are resonating. The worst case scenario is not easy to determine with such EUT. As we could not perform a n observation test in a FAR, we performed five measurements in the GTEM cell by changing the orientation of the EUT.

A schematic of the electronic circuit is given in figure 12. A voltage $V_i = 2.70$ V is supplied to the 8 bits ADC. We observe the voltage V_s at the least significant pin. A failure is observed when the value of V_s changes from 0 to 1. The

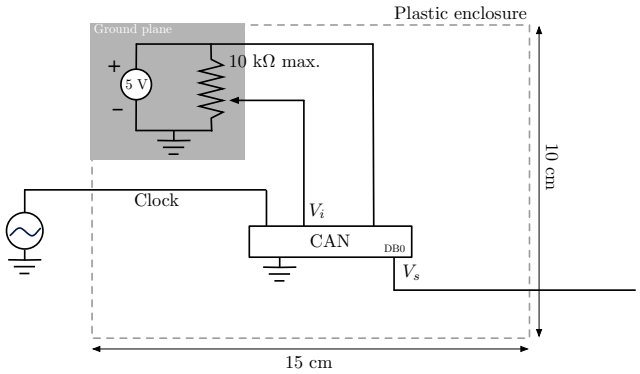

Fig. 12. Schematic view of the complex EUT's electronic board.

failure can either correspond to a 0.02 V variation of the input voltage V_i or an internal failure of the ADC. The binary value of the output voltage is stored.

B. Modus operandi

The measurements are performed between 850 MHz and 1500 MHz. At these frequencies, the behavior of our RC is ideal and measurements have shown that the rectangular components of the E-field follow a Rayleigh distribution. We choose to use $n = 150$ stirrer positions and the power injected in the chamber is increased gradually allowing to reach a magnitude of 110 V.m^{-1} for the mean value of the rectangular components of the E-field. Susceptibility measurements were performed with the same setup in a GTEM cell, the maximum E-field magnitude reached in the GTEM cell was around 100 V.m^{-1}

We perform measurements in a GTEM cell and in an RC with both EUTs. Only one measurement is performed in the GTEM cell with the simple EUT as we can assume that we get the worst case scenario when the antenna is vertical. With the complex EUT however, due to the multiple coupling paths, we perform five measurements with different orientations.

In the RC, we perform measurements with both the IEC standard [3] and our binomial approach. The standard approach is based on a statistical estimation of the maximum E-field (or power) one could expect for a given number of observations n and a given power injected in the chamber. One assumes that this estimated maximum E-field creates a failure on the EUT. The estimation of the maximum is a topic of interest in the RC community [3], [19]–[22]. The statistical uncertainty of this estimation can be important and the correlation between measurements performed in a deterministic environment like a GTEM cell and in an RC can be difficult to establish.

C. Results

1) simple EUT: Figure 13-(a) shows the immunity measurements results on the EUT with the op-amp. This figure shows clearly a good agreement between the measurement performed in the GTEM cell and in the RC according to the binomial approach. The estimation of the the immunity

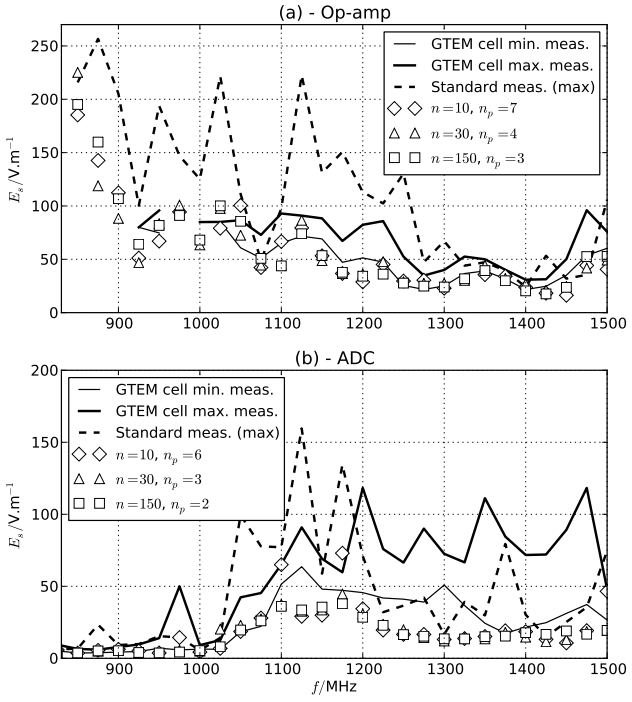

Fig. 13. Immunity measurements performed in a GTEM cell and in an RC with both the IEC standard approach and our binomial approach.

based on the IEC standard with $n = 150$ stirrer positions exhibits oscillations. These oscillations are of statistical nature and can overestimate the linear immunity of the EUT by a factor 4 for certain frequencies (a 12 dB difference in terms of power). This figure shows that increasing the number of stirrer positions n does not significantly improve the statistics of the estimation. With $n = 10$, the estimation is slightly more spread. The number of power levels tested n_p during the measurements decrease with n. With $n = 10$, 7 power levels chosen according (11) are necessary to get a complete picture of the immunity of the EUT. With $n = 30$, n_p reduces to four power levels and with $n = 150$, only 3 power levels are needed. Reducing the number of power levels n_p tested when increasing the number of observations n allows to slightly decrease the duration of the test as shown empirically in [23].

2) Complex EUT: Figure 13-(b) shows the results observed with the complex EUT. Starting from 1 GHz, the EUT is electrically large enough to resonate and to present multiple coupling paths. This can explain the spread of the immunity levels for the five measurements in the GTEM cell. Under 1 GHz, measurements performed with the GTEM cell and in the RC are in good agreement. Above 1 GHz, the radiation pattern of the EUT starts to be complex and the GTEM cell gives different immunity levels for every measurement. Measurements performed in the RC according the standard look less erratic even if the statistical uncertainty for estimating the maximum creates some oscillations. The values obtained with the binomial approach are in good agreement with the GTEM measurements if we consider the minimum value of the five measurements. With this EUT, it is highly probable that the failures observed are created by a simultaneous illumination of different coupling paths. The comparison of measurements performed in the GTEM cell and in the reverberation is not straightforward as the number of coupling paths illuminated for each is not known. These results show that a good agreement can be found if we use a binomial approach to extract the susceptibility level from the measurements performed in the RC.

D. Interpretation

These measurements performed in a GTEM cell, and in an RC according both the IEC standard and our binomial approach give a good idea of the advantages and the drawbacks of each approach with simple or complex EUTs.

With simple EUTs, for which the worst case scenario (maximum coupling configuration) is clearly identified, deterministic measurements with plane waves would give accurate immunity measurements with few observations. A deterministic environment is more straightforward for such EUTs. These measurements show that the binomial approach applied to measurements performed in an RC gives very similar results with as few as $n = 10$ stirrer positions.

With complex EUTs however, the measurements show that an RC provide a safer test by illuminating multiple coupling paths simultaneously. The binomial model allows to access the immunity level with a good accuracy with very few observations and may be a more accurate and time saving alternative to the standard measurement [3].

VI. Conclusion

This article proposes a new theoretical framework for EMC tests. Our goal is to provide a general paradigm that allows to extract immunity levels from the binomial statistics of the tests testing performed with plane waves environments or random field environments. We show that this approach is suitable for any immunity testing in random fields as well as tests in plane wave environments as long as the EUT provides a statistical dimension to the test.

We show that this binomial approach to immunity measurements in EMC allows to control the uncertainty of the estimation. A typical 3 dB uncertainty budget on a power estimation can be achieved with as few as $n = 10$ observations. We establish a relation between the number of observations n and the number of power levels tested n_p. We derive an optimal number of power levels tested and thus improve the duration of the test. Numerical simulations and measurements show that the uncertainty is indeed well controlled and measurements in an RC and in a deterministic environment are in good agreement with this approach.

Further investigations could be to validate this approach by measuring the immunity of electrically large and complex EUTs in a FAR and compare the results with measurements in an RC. As long as the statistic properties of the radiation pattern of the EUT are well known [17], we are very confident about the forthcoming results.

The probability of failure is a quantity commonly used to study the reliability of systems and their functional safety [24]. If the EUT can be described by a set of functions. This

approach could measure the susceptibility level and the probability of failure of each function. We could verify if the EUT's reliability is in agreement with the designed behavior. The immunity testing could test both the EMC of the EUT and its reliability. Such double test could be of interest for the automotive [25] and the aerospace industry [26].

APPENDIX A
ALTERNATIVE PROOF THAT A COMPLEX EUT MAY RADIATE AN E-FIELD WITH RAYLEIGH DISTRIBUTED RECTANGULAR COMPONENTS

The EUT is modelled by a sphere of radius r. n hertzian dipoles with random moment $\vec{\mu}$ (uniform distribution between 0 and 1) and random phase (uniform distribution between 0 and 2π) are placed randomly on the surface of the sphere, with random angular orientation. Such random EUTs are commonly used in the literature [7], [27].

The superposition of the contribution of each dipole in the EUT in the far-field can be described with two orthogonal components. We consider the E-field on a sphere of radius R with $R \gg 2r^2/\lambda$. If we use the usual local spherical coordinates system $(\vec{e}_r, \vec{e}_\theta, \vec{e}_\phi)$, we neglect the radial component $\vec{e}_r$. It two dimensions random walk with $\langle||\vec{\mu}||\rangle$ average displacement. The magnitude of each complex component of the E-field follows a normal distribution with zero mean and with variance:

$$\sigma^2 \quad = \quad n\left(\frac{\langle||\vec{\mu}||\rangle}{R}\right)^2 = \frac{n}{4R^2} \tag{12}$$

We can write the resulting complex E-field:

$$E = \mathcal{N}(0,\sigma^2) + j\mathcal{N}(0,\sigma^2) \tag{13}$$

In far field, we only consider the transverse components E_θ and E_ϕ:

$$E_\theta = E_{\theta_r} + jE_{\theta_i} \text{ and } E_\phi = E_{\phi_r} + jE_{\phi_i} \tag{14}$$

with,

$$\langle E_{\theta_r}\rangle = \langle E_{\theta_i}\rangle = \langle E_{\phi_r}\rangle = \langle E_{\phi_i}\rangle = 0 \tag{15}$$

and their variances are:

$$\langle E^2_{\theta_r}\rangle = \langle E^2_{\theta_i}\rangle = \langle E^2_{\phi_r}\rangle = \langle E^2_{\phi_i}\rangle = \frac{\sigma^2}{4} \tag{16}$$

The magnitudes of the components E_θ and E_ϕ follow a Rayleigh distribution with parameter $\beta = \sigma/2$. We can derive that the power emitted follows an exponential distribution [8]. This result is in agreement with [17].

REFERENCES

[1] *IEC 61000-4-22 Ed. 1 (CDIS)(CISPR/A):Electromagneticcompatibil- ity (EMC)—part 4.21: Testing and measurement techniques — radiated emissions and immunity measurements in fully anechoic rooms (FARs),*, IEC, Geneva, Switzerland, Nov. 2010.

[2] *IEC 61000-4-20 Ed. 2 (joint task force IEC SC77B-CISPR/A): Electromagnetic compatibility (EMC)—part 4.20: Testing and measurement techniques — emission and immunity testing in transverse electromagnetic (TEM) waveguides*, IEC, Geneva, Switzerland, Sep. 2010.

[3] *IEC 61000-4-21 Ed. 2 (joint task force IEC SC77B-CISPR/A): Electromagnetic compatibility (EMC)—part 4.21: Testing and measurement techniques — reverberation chamber test methods*, IEC, Geneva, Switzerland, Feb. 2010.

[4] L. Jansson and M. Backstrom, "Directivity of equipment and its effect on testing in mode-stirred and anechoic chamber," in *Electromagnetic Compatibility, 1999 IEEE International Symposium on*, vol. 1, 1999, pp. 17 – 22.

[5] T. Harrington, "Total-radiated-power-based oats-equivalent emissions testing in reverberation chambers and gtem cells," in *Electromagnetic Compatibility, 2000. IEEE International Symposium on*, vol. 1, 2000, pp. 23 – 28.

[6] L. Musso, F. Canavero, B. Demoulin, and V. Berat, "Radiated immunity testing of a device with an external wire: repeatability of reverberation chamber results and correlation with anechoic chamber results," in *Electromagnetic Compatibility, 2003 IEEE International Symposium on*, vol. 2, aug. 2003, pp. 828 – 833.

[7] H. Krauthäuser, "Statistical analysis of the correlation of emission limits for established and alternative test sites," *Electromagnetic Compatibility, IEEE Transactions on*, vol. 53, no. 4, pp. 863 – 875, nov. 2011.

[8] A. Papoulis, *Probability, Random Variables, and Stochastic Processes*, 4th ed. New York: Mc Graw Hill, 2002.

[9] P.-S. Laplace, *Théorie analytique des probabilités*. Paris: Courcier, 1812.

[10] C. J. Clopper and E. S. Pearson, "The use of confidence or fiducal limits illustrated in the case of the binomial," *Biometrika*, vol. 26, no. 4, pp. 404 – 413, 1934.

[11] A. Agresti and B. A. Coull, "Approximate is better than "exact" for interval estimation of binomial proportions," *The American Statistician*, vol. 52, no. 2, pp. 119 – 126, 1998.

[12] E. B. Wilson, "Probable inference, the law of succession, and statistical inference," *Journal of the American Statistical Association*, vol. 22, no. 158, pp. 209 – 212, 1927.

[13] L. D. Brown, T. T. Cai, and A. DasGupta, "Interval estimation for a binomial proportion," *Statist. Sci.*, vol. 16, no. 2, pp. 101 – 133, 2001.

[14] T. D. and Ross, "Accurate confidence intervals for binomial proportion and poisson rate estimation," *Computers in Biology and Medicine*, vol. 33, no. 6, pp. 509 – 531, 2003.

[15] T. Lehman and E. Miller, "The statistical properties of electromagnetic fields with application to radiation and scattering," in *Antennas and Propagation Society International Symposium, 1991. AP-S. Digest*, vol. 3, Jun. 1991, pp. 1616 – 1619.

[16] J. Kostas and B. Boverie, "Statistical model for a mode-stirred chamber," *Electromagnetic Compatibility, IEEE Transactions on*, vol. 33, no. 4, pp. 366 – 370, Nov. 1991.

[17] M. Hoijer, "Maximum radiated power density from electrically large sources; comparing probability theory and measurements," *Electromagnetic Compatibility, IEEE Transactions on*, vol. 53, no. 4, pp. 876 – 881, nov. 2011.

[18] Y. He and A. Marvin, "Aspects of field statistics inside nested frequency-stirred reverberation chambers," in *Electromagnetic Compatibility, 2009. EMC 2009. IEEE International Symposium on*, aug 2009, pp. 171 – 176.

[19] T. Lehman and G. Freyer, "Characterization of the maximum test level in a reverberation chamber," in *Electromagnetic Compatibility, 1997. IEEE 1997 International Symposium on*, Aug. 1997, pp. 44 – 47.

[20] K. Harima, "Statistical characteristics of maximum E-field distribution in a reverberation chamber," in *Electromagnetic Compatibility, 2004. EMC 2004. 2004 International Symposium on*, vol. 2, Aug. 2004, pp. 724 – 727.

[21] G. Orjubin, "Maximum field inside a reverberation chamber modeled by the generalized extreme value distribution," *Electromagnetic Compatibility, IEEE Transactions on*, vol. 49, no. 1, pp. 104 – 113, Feb. 2007.

[22] A. Gifuni, "Deterministic approach to estimate the upper bound of the electric field in a reverberation chamber," *Electromagnetic Compatibility, IEEE Transactions on*, vol. 53, no. 3, pp. 570 – 578, aug. 2011.

[23] E. Amador, C. Lemoine, and P. Besnier, "Optimization of immunity testings in a mode tuned reverberation chamber with Monte Carlo simulations," in *Proceedings of the 2012 ESA Workshop on Aerospace EMC in Venice*, 2012, pp. 1 – 6.

[24] *IEC 61508 – Functional safty of electrical/electronic/programmable electronic safey-related systems (7 parts)*, IEC, Geneva, Switzerland.

[25] S. Alexandersson, "Functional safety and EMC for the automotive industry," in *Electromagnetic Compatibility, 2008. EMC 2008. IEEE International Symposium on*, aug. 2008, pp. 1 –6.

[26] *RTCA DO-254/Eurocae ED-80 "Design assurance guidance for airborne electronic hardware"*, RTCA—RTCA Inc. and EUROCAE.

[27] P. Wilson, D. Hill, and C. Holloway, "On determining the maximum emissions from electrically large sources," *Electromagnetic Compatibility, IEEE Transactions on*, vol. 44, no. 1, pp. 79 – 86, feb 2002.

Emmanuel Amador received the Dipl.Ing. degree from Telecom SudParis, Evry, France, in 2006, the M.Sc. degree in electrical engineering from Laval University, Québec City, Canada, in 2008 and his Ph.D. degree in electronics in 2011 from the National Institute of Applied Sciences (INSA) in Rennes, France.

In November 2011, he was a visiting researcher at the electromagnetic theory and compatibility chair at Technical University Dresden, Dresden, Germany. Since October 2012, he has been a Research Engineer in the EMC lab with EDF R&D, France. His current research interests include reverberation chambers, statistical electromagnetic, electromagnetic compatibility of complex systems and lightning protection.

Hans Georg Krauthäuser (M98 – SM11) received the Diploma degree (M.S.) in physics and the Doctorate degree (Ph.D.) both from the University of Cologne, Cologne, Germany, in 1992 and 1996, respectively.

From 1997 to 2008, he was a Research Assistant and an Assistant Lecturer at the Otto-von-Guericke University Magdeburg, Magdeburg, Germany. Since 2008, he has been a Full Professor in electromagnetic theory and compatibility at Technical University Dresden, Dresden, Germany. His main research interests include reverberation chambers, statistical electromagnetics, electromagnetic interactions with complex systems, measurement technology, and inverse scattering problems.

Dr. Krauthäuser is member of IEEE Electromagnetic Compatibility Society, Union Radio-Scientifique Internationale (Commission E) and Association for Electrical, Electronic and Information Technologies. He is active in the development of IEC 61000-4-20 and -21 in national working groups and in the CISPR/A-IEC/SC77B Joint Task Forces on reverberation chambers.

Philippe Besnier (SM10) received the diplôme d'ingénieur degree from Ecole Universitaire d'Ingénieurs de Lille (EUDIL), Lille, France, and the Ph.D. degree in electronics from the University of Lille, Lille, France, in 1990 and 1993, respectively.

Following a one-year period at ONERA, Meudon, as an Assistant Scientist in the EMC Division, he was with the Laboratory of Radio Propagation and Electronics, University of Lille, as a Researcher at the Centre National de la Recherche Scientifique (CNRS) from 1994 to 1997. From 1997 to 2002, he was the Director of Centre d'Études et de Recherches en Protection Électromagnétique (CERPEM), a nonprofit organization for research, expertise, and training in EMC, and related activities, based in Laval, France. He cofounded TEKCEM in 1998, a private company specialized in turnkey systems for EMC measurements. Since 2002, he has been with the Institute of Electronics and Telecommunications of Rennes, Rennes, France, where he is currently a Researcher at CNRS heading EMC-related activities such as EMC modeling, electromagnetic topology, reverberation chambers, and near-field probing.